

# RESEARCH ACTIVITIES V

## Department of Applied Molecular Science

### V-A Synthesis of Chiral Molecule-Based Magnets

Construction of molecule-based magnetic materials, which have additional properties such as conductivity or photo reactivity, is now becoming a challenging target. Specific goals aimed for these molecule-based magnets include: i) the ability to design the molecular building blocks and to organize them in the solid for desired dimensionality, ii) the optical transparency. The physical characteristic of current interest involves optical properties, particularly with respect to natural optical activity. When a magnet has optical transparency and chiral structure, the magnetic structure of crystal expects to be a chiral spin structure. These magnets will show an asymmetric magnetic anisotropy and magneto-chiral dichroism. This category of materials don't only have scientific interest but also have the possibility for use in new devices. When we construct chiral molecule-based magnets, chirality must be controlled not only in the molecular structure, but in the entire crystal structure. As a consequence of this difficulty, only few examples of this type of magnet exist. Up to the present reported chiral magnets have low dimensional magnetic structures, the magnetic ordering temperatures are below 10 K. To afford a high- $T_C$  magnet, dimensionality of magnetic structure must be extended in two or three dimension. When we introduce magnetic bricks, which have more than three connections for the construction of magnets, we can expect to make two or three-dimensional magnets. To make high dimensionality molecule-based magnets, we recently discovered using cyano bridged complex with chiral organic ligands.

#### V-A-1 A Novel Two-Dimensional Chiral Complex; $[\text{Cu-II}(R)\text{-pn}]_2[\text{Ni-II}(\text{CN})_4]_2 \cdot \text{H}_2\text{O}$ ( $(R)\text{-pn} = (R)\text{-1,2-Diaminopropane}$ )

IMAI, Hiroyuki; INOUE, Katsuya; OHBA, Masaaki<sup>1</sup>; OKAWA, Hisashi<sup>1</sup>; KIKUCHI, Koichi<sup>2</sup>  
(<sup>1</sup>Kyushu Univ.; <sup>2</sup>IMS and Tokyo Metropolitan Univ.)

[*Synth. Met.* **137**, 919–920 (2003)]

The synthesis, single crystal X-ray structures and magnetic properties of a new two-dimensional chiral complex;  $[\text{Cu-II}(R)\text{-pn}]_2[\text{Ni-II}(\text{CN})_4]_2 \cdot \text{H}_2\text{O}$  ( $(R)\text{-pn} = (R)\text{-1,2-diaminopropane}$ ), are described. Blue plate crystals of  $[\text{Cu-II}(R)\text{-pn}]_2[\text{Ni-II}(\text{CN})_4]_2 \cdot \text{H}_2\text{O}$  were obtained by the reaction between  $[\text{Cu}(R)\text{-pn}](\text{SO}_4)$  and  $\text{K}_2[\text{Ni}(\text{CN})_4]$  in  $\text{H}_2\text{O-EtOH}(1:1)$ . The structures consist of a two-dimensional cyano-metal network as shown in Figure 1 and 2. The temperature dependence of  $\chi T$  is shown in Figure 3. At low temperature  $\chi T$  decreases with lowering temperature. This tendency indicates a weak antiferromagnetic interaction dominates between copper ions. The magnetic susceptibility of this crystals can be reproduced by Curie-Weiss law with the parameters of  $C = 0.849 \text{ emu K mol}^{-1}$  ( $g = 2.2$ ) and  $\theta = -1.27 \text{ K}$ .

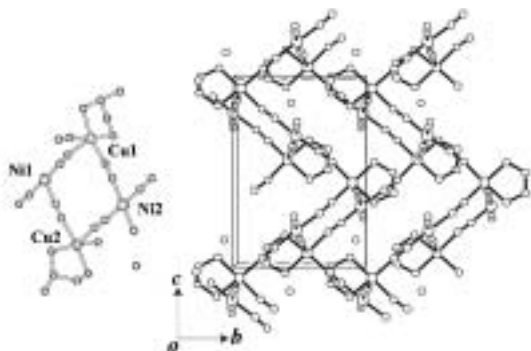


Figure 1. The asymmetric unit of  $[\text{Cu}^{\text{II}}(R)\text{-pn}]_2[\text{Ni}^{\text{II}}(\text{CN})_4]_2 \cdot \text{H}_2\text{O}$  and the two-dimensional chiral network in the  $bc$ -plane.

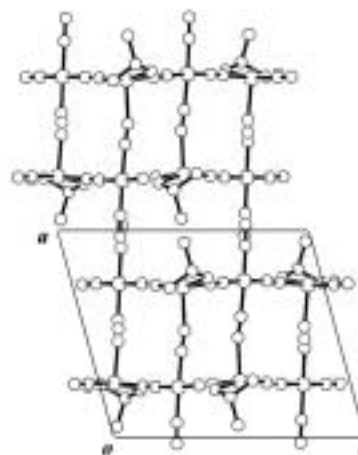


Figure 2. The side view of the two-dimensional sheet along  $b$ -axis.

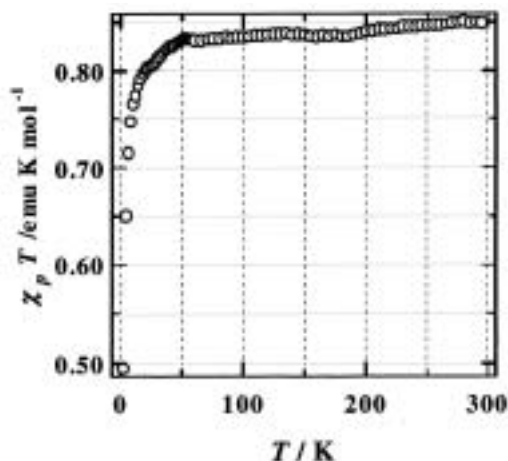


Figure 3. The temperature dependence of the  $\chi T$ .

## V-B Hydrothermal Synthesis of Molecule-Based Magnets

Coordination polymers are attracting much interest due to the strength and rigidity of the extended lattices for gas absorption and intercalation and for the connectivity between magnetic ions in designing molecule-based magnets. They belong to a subset of organic-inorganic hybrid materials, and usually employ a central metal ion and a multitopic organic ligands or a coordination complex having ambidentate ligands, such as cyanide and oxalate. In some cases, other organic ligands are used to control the dimensionality or structure. The choice of the metals and of the ligands depends on the desired properties. On the one hand, there is strong interest by scientists studying catalysis and the absorption of gases originating from the possibility of creating structures with cavities, channels or pores and, consequently, large surface areas. On the other hand, there is increasing interest from magneto-chemists due principally to the realization of organizing the magnetic orbitals of the moment carriers to favor a particular magnetic ground state. The field of coordination polymers based on organic radicals is a very active area, indeed. Several ground states have been established and a clear molecular-orbital picture to explain the observations is emerging. For the realizing strong magnetic interaction, it is better to use simple and small organic ligands, such as cyanide or carboxylate ions. The metal complexes with such ligands are usually less solvability. The thermal synthesis is powerful method to make large single crystals for such complexes.

### V-B-1 Synthesis and Characterization of One-Dimensional Mixed-Spin Cobalt(II) Metamagnet

OKA, Yoshimi; KUMAGAI, Hitoshi; INOUE, Katsuya

The hydrothermal synthesis, single crystal X-ray analysis and magnetic properties of a one-dimensional mixed-spin  $\text{Co}^{\text{II}}$  Metamagnet,  $[\text{Co}_4(\text{phcina})_6(\text{OH})_2(\text{H}_2\text{O})_4] \cdot 2\text{H}_2\text{O}$  (phcina = alpha-phenylcinnamate), is described. Pink needle crystals of  $[\text{Co}_4(\text{phcina})_6(\text{OH})_2(\text{H}_2\text{O})_4] \cdot 2\text{H}_2\text{O}$  was obtained at 120 °C. The x-ray structure analysis of **1** revealed the formation of 1-D chain along the *c*-crystal axis. (Figure 1 and 2). The asymmetric unit consists of two distorted octahedral  $\text{Co}^{\text{II}}$  ions (Co(1), Co(3)) and two octahedral  $\text{Co}^{\text{II}}$  ions (Co(2), Co(4)). Co(2) and Co(4) exhibit octahedral geometry comprising of three oxygen atoms of phcina ligands, one hydroxide and two waters. The O–Co–O bond angles in the  $\{\text{CoO}_6\}$  octahedral site range from 81.37(8) ° to 98.18(10) ° and bond distances range from 2.029(2) to 2.163(3) Å (*av.* 2.10 Å). These values are similar to that found in octahedral  $\text{Co}^{\text{II}}(\text{HS})$  complexes. In contrast, Co(1) and Co(3) exhibit distorted octahedral geometry, pseudo  $C_{4v}$  symmetry comprising of three oxygen atoms of phcina ligands, two hydroxides and one water. Co(1) has O(2), O(7), O(9) and O(15) in the basal plane and these O–Co(1)–O angles range from 82.16(10) ° to 94.37(10) °. These configurations are similar that found in  $\text{Co}^{\text{II}}(\text{LS})$  complexes. The nearest intermetallic separation between  $\text{Co} \cdots \text{Co}$  along *b*-axis is 3.095(2) Å and that along *a*- or *c*-axis is more than 14.406(4) Å. Figure 3 shows the temperature dependence of the magnetic susceptibility, the product of susceptibility and temperature and inverse susceptibility. The  $\chi T$  value is 9.87 emu K mol<sup>-1</sup> at 300 K and reaches a local minimum at 35 K (7.18 emu K mol<sup>-1</sup>) and then rapidly increases. The effective magnetic moment ( $\mu_{\text{eff}}$ ) per four cobalt ions is 9.87  $\mu_B$  at room temperature which is consistent with that expected for four  $\text{Co}^{\text{II}}(\text{HS})$  ions. It is indicative that the value 7.58  $\mu_B$  of  $\mu_{\text{eff}}$  at 35 K is assigned to two distorted octahedral  $\text{Co}^{\text{II}}(\text{LS})$  and two octahedral  $\text{Co}^{\text{II}}(\text{HS})$  ions, this complex shows gradual spin-crossover behavior of  $\text{Co}^{\text{II}}$  with  $C_{4v}$  symmetry and orbital contribution through spin-

orbit coupling of octahedral  $\text{Co}^{\text{II}}$  ions as temperature increases. High-spin  $\text{Co}^{\text{II}}$  ions and low-spin  $\text{Co}^{\text{II}}$  ions interact ferrimagnetically and ferrimagnetic chains interact antiferromagnetically below  $T_N = 5.5$  K. (Figure 4)

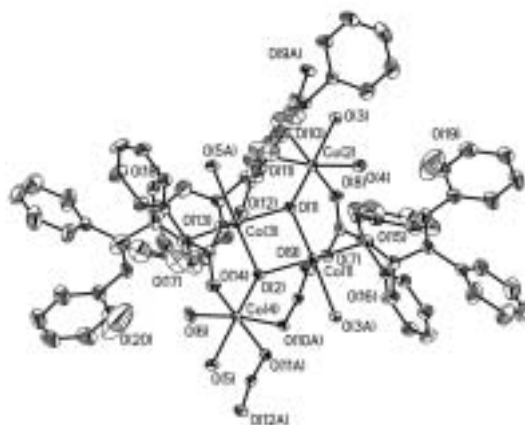


Figure 1. X-ray crystal structure of **1**.

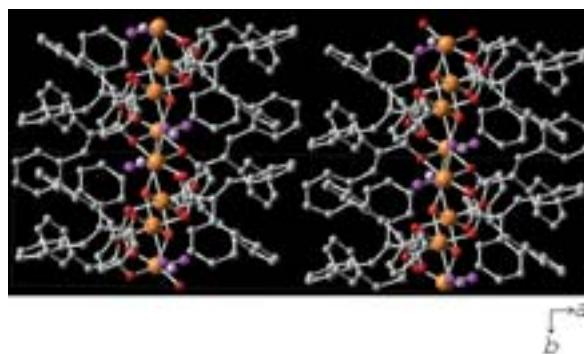
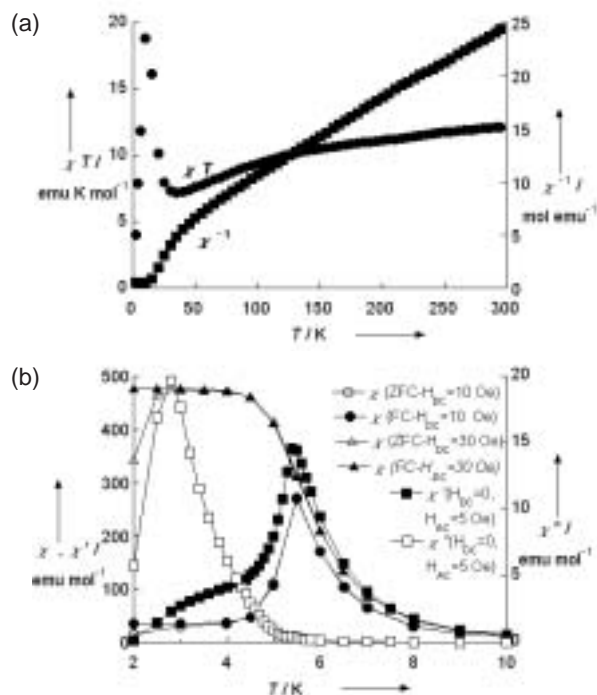
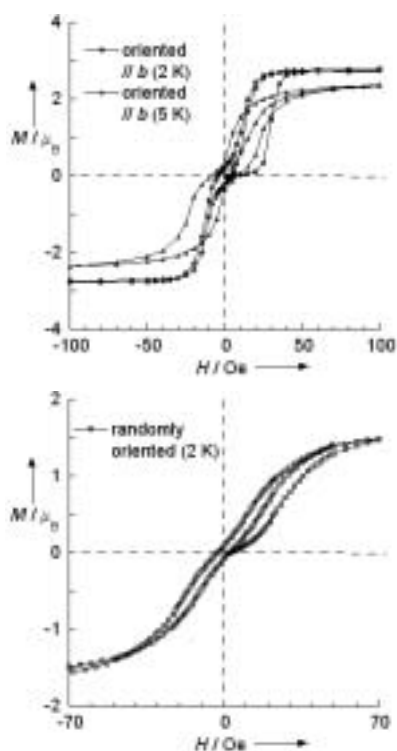


Figure 2. Packing diagram of the 1-D chain compound **1** along *c*-axis. Orange, red, dark red, purple, pink and gray represented Co, O(hydroxo), O(carboxylate), O(coordinated water), O(crystal water) and C, respectively.



**Figure 3.** (a) Magnetic susceptibility of randomly oriented polycrystalline sample represented as  $\chi T$  and  $\chi^{-1}$  per 4 Co ions. The applied field was 5 kOe. (b) Temperature dependence of the magnetic susceptibilities per 4 Co ions for oriented polycrystalline sample along  $b$ -axis. The applied DC field was 10 Oe and 30 Oe, and ZFC and FC refer to zero-field cooled and field-cooled, respectively. AC magnetic susceptibilities are also shown when applied DC field is 0 with AC field of 5 Oe and AC frequency of 1 Hz.



**Figure 4.** (a) Hysteresis loops for oriented polycrystalline sample along  $b$ -axis at 2 K and 5 K. (b) Hysteresis loop for randomly oriented sample at 2 K. Magnetic field was up to 70 kOe and magnetization values per 4 Co ions are shown.

## V-B-2 Hydrothermal Synthesis, Structure and Magnetism of Square-Grid Cobalt(II)-Carboxylate Layered Compounds with and without Pillars

KUMAGAI, Hitoshi<sup>1</sup>; OKA, Yoshimi; INOUE, Katsuya; KURMOO, Mohamedally<sup>2</sup>  
 (<sup>1</sup>IMS and Inst. Phys. Chem. Materials Strasbourg, France; <sup>2</sup>Inst. Phys. Chem. Materials Strasbourg, France)

[*J. Chem. Soc., Dalton Trans.* 3442–3446 (2002)]

The hydrothermal synthesis, single crystal X-ray structures and magnetic properties of two layered cobalt(II)-carboxylate complexes,  $[\text{Co}^{\text{II}}(\text{H}_2\text{O})_2(\text{O}_2\text{C}-\text{CHCHC}_6\text{H}_5)_2]$  (**1**) and  $[\text{Co}^{\text{II}}(\text{H}_2\text{O})_2(\text{O}_2\text{CCHCHC}_6\text{H}_4\text{CO}_2)_{2/2}]$  (**2**), are described. Pale red crystals of  $\text{Co}(\text{H}_2\text{O})_2\text{L}_2$ ,  $\text{L} = \text{trans-cinnamate} (\text{C}_9\text{H}_7\text{O}_2^-)$  (**1**) or  $\text{L}_2 = 4\text{-carboxycinnamate} (\text{C}_{10}\text{H}_6\text{O}_4^{2-})$  (**2**), were obtained at 120 °C. The structures consist of square-grid 2D-coordination polymeric sheets,  $\cdots-\text{OCO}-\text{Co}(\text{H}_2\text{O})_2-\text{OCO}-\text{Co}(\text{H}_2\text{O})_2-\cdots$ , separated by  $\text{C}_6\text{H}_5-\text{CH}=\text{CH}-$  for (**1**) or pillared by  $-\text{C}_6\text{H}_4-\text{CH}=\text{CH}-$  for (**2**). (Figure 1, 2 and 3) The magnetism was studied as a function of temperature and magnetic field. In both cases the magnetic moment decreases on lowering the temperature due to spin-orbit coupling and no interaction between cobalt ions. The data can alternatively be fitted to an unrealistic quadratic layer model for  $S = 3/2$  without taking into account the effect of spin-orbit.

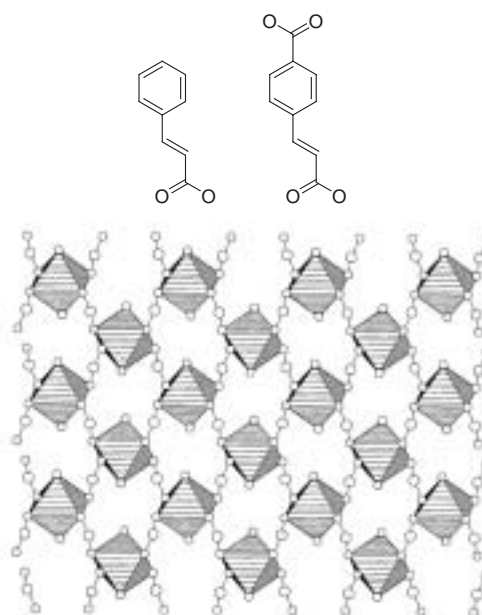


**Figure 1.** Crystal structure of **1** and **2** along  $a$  axis.

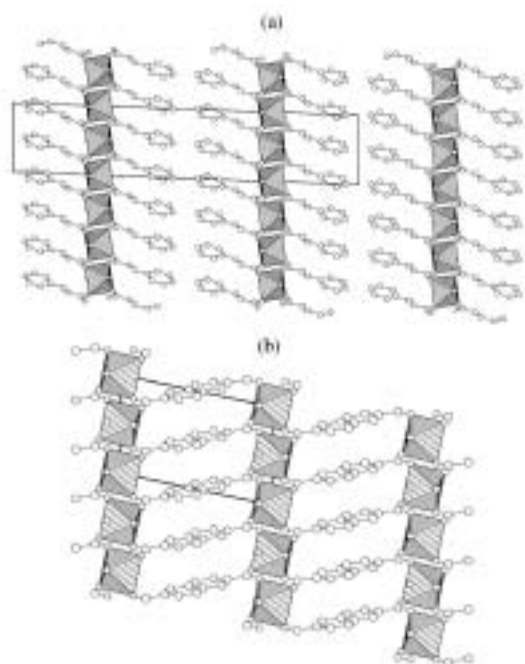


**Figure 2.** View of the *ab* plane arrangement of the organic backbone in the galleries in **1** (a) and **2** (b).

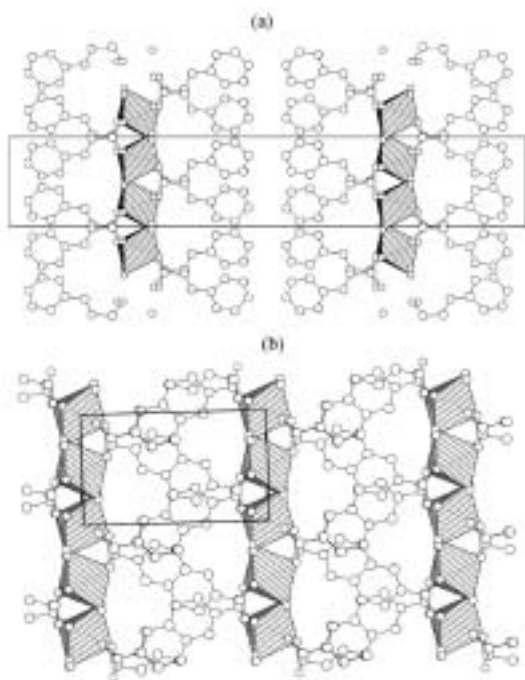


**Figure 3.** View of the *ac* plane arrangement of the organic backbone in the galleries in **1** (a) and **2** (b).

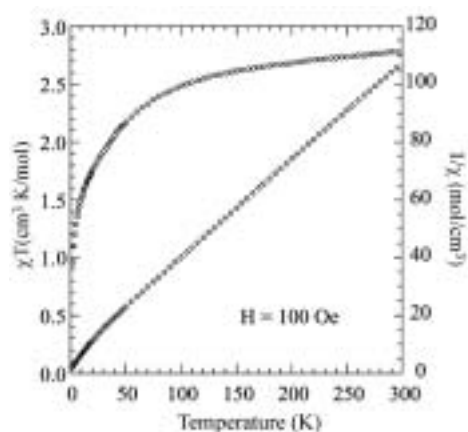


**Figure 4.** Temperature dependence of the product of susceptibility and temperature (circles) and the inverse susceptibility for **2** (diamonds).

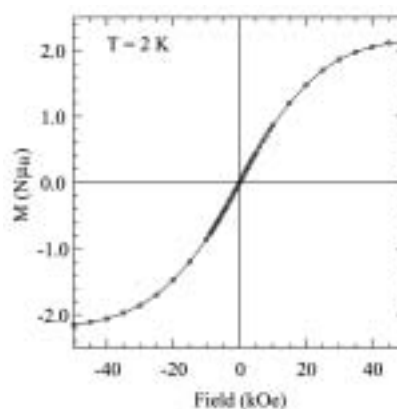


**Figure 5.** Isothermal magnetization of **2** at 2 K; line is a guide to the eye.